Astron. Astrophys. 341, 539–546 (1999)

ASTRONOMY
AND
ASTROPHYSICS

High-resolution abundance analysis of two individual stars of the bulge globular cluster NGC 6553⋆

B. Barbuy[1], **A. Renzini**[2], **S. Ortolani**[3], **E. Bica**[4], **and M.D. Guarnieri**[2]

[1] Universidade de São Paulo, CP 3386, São Paulo 01060-970, Brazil
[2] European Southern Observatory, Karl-Schwarzschild Strasse 2, D-85748 Garching bei München, Germany
[3] Università di Padova, Dept. di Astronomia, Vicolo dell'Osservatorio 5, I-35122 Padova, Italy
[4] Universidade Federal do Rio Grande do Sul, Dept. de Astronomia, CP 15051, Porto Alegre 91500-970, Brazil

Received 14 August 1998 / Accepted 22 September 1998

Abstract. A detailed abundance analysis of 2 giants of the metal-rich bulge globular cluster NGC 6553 was carried out using high resolution échelle spectra obtained at the ESO 3.6m telescope.

The temperature calibration of metal-rich cool giants needs high quality photometric data. We have obtained JK photometry at ESO and VI photometry with the Hubble Space Telescope for NGC 6553. The main purpose of this analysis consists in the determination of elemental abundance ratios for this key bulge cluster, as a basis for the fundamental calibration of metal-rich populations. The present analysis provides a metallicity [Fe/H] = -0.55 ± 0.2 which, combined to overabundances relative to Fe of several elements, results in an overall metallicity Z $\approx$ Z$_\odot$.

Key words: stars: abundances – Galaxy: globular clusters: individual: NGC 6553

1. Introduction

The metal-rich bulge globular clusters are a keystone for the understanding of the formation of the Galactic bulge, which in turn has consequences on the scenarios of galaxy formation.

Globular clusters in the Galactic bulge form a flattened system, extending from the Galactic center to about 4.5 kpc from the Sun (Barbuy et al. 1998). A study of abundance ratios in these clusters is very important for better understanding the formation of the Galactic bulge. The interest in NGC 6553 resides on its location at d$_\odot$ $\approx$ 5.1 kpc, therefore relatively close the sun, and at the same time it is representative of the Galactic bulge stellar population: (a) Bica et al. (1991) and Ortolani et al. (1995) showed that NGC 6553 and NGC 6528 present very similar Colour-Magnitude Diagrams (CMDs), and NGC 6528 is located at d$_\odot$ $\approx$ 7.83 kpc in the Baade Window, very close to the Galactic center; (b) the stellar population of the Baade Window is very similar to that of NGC 6553 and NGC 6528 as shown by Ortolani et al. (1995) by comparing their CMDs and luminosity functions, indicating that they have comparable metallicity and age.

One fundamental issue concerns the star formation timescale in the bulge, the age of bulge stars, and its signature through elemental abundance ratios. A first answer to these questions was given by Ortolani et al. (1995) where it was revealed that the bulge clusters NGC 6528 and NGC 6553 are nearly coeval to the halo clusters. The final value of the ages still depends on the relation between absolute magnitude of horizontal branch (HB) stars and metallicity.

In this work, we address the question of element abundances, in particular the α/Fe ratio in bulge globular clusters. For Baade's Window field stars McWilliam & Rich (1994, hereafter MR) have determined ratios [Mg/Fe] $\approx$ [Ti/Fe] $\approx$ +0.3 and [Ca/Fe] $\approx$ [Si/Fe] $\approx$ 0.0. From low-resolution spectra for 400 Baade's Window stars, Sadler et al. (1996) have found [Mg/Fe] $\approx$ 0.3, whereas Idiart et al. (1996) obtained [Mg/Fe] $\approx$ +0.45 from an integrated spectrum of Baade's Window.

No determination of such abundances in metal-rich bulge clusters is yet available. In Barbuy et al. (1992) the giant member star III-17 was analysed, where [Fe/H] ≈ -0.2 was obtained; no abundance ratios had been derived due to limitations in S/N.

In this work we present detailed abundance analyses of 2 stars in NGC 6553 using high resolution échelle spectra obtained at the ESO 3.6m telescope. We also discuss this cluster as a calibrator of the metallicity scale of globular clusters.

In Sect. 2 the observations are described. In Sect. 3 the stellar parameters effective temperature, gravity, metallicity and abundance ratios are derived. In Sect. 4 the results are discussed. In Sect. 5 conclusions are drawn.

2. Observations

High resolution observations of individual stars of NGC 6553, located at α_{1950} = $18^h05^m11^s$, δ_{1950} = -25^o55'06", were obtained at the 3.6m telescope of the European Southern Observatory – ESO. The Cassegrain Échelle Spectrograph (CASPEC) was used with a thinned and anti-reflection coated Tektronix CCD of 512x512 pixels, of pixel size 27x27μm (ESO # 32). The 31.6 gr/mm grating was used with the short camera and the

⋆ Observations collected at the European Southern Observatory – ESO, Chile

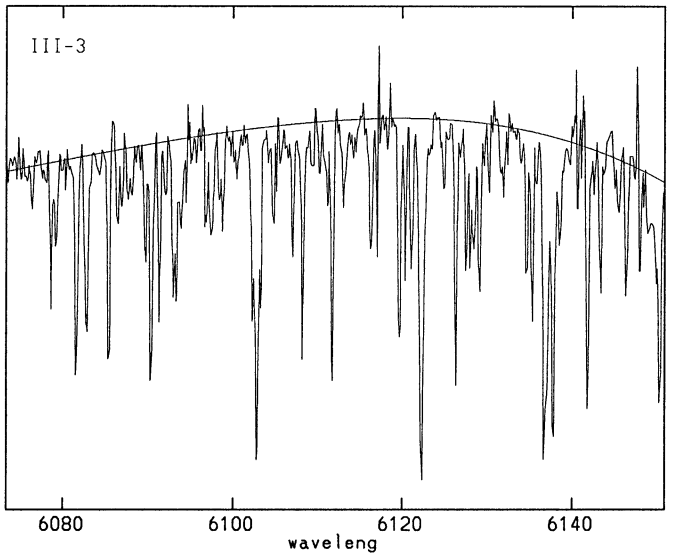

Fig. 1. Typical spectrum of the star III-3 (order 93)

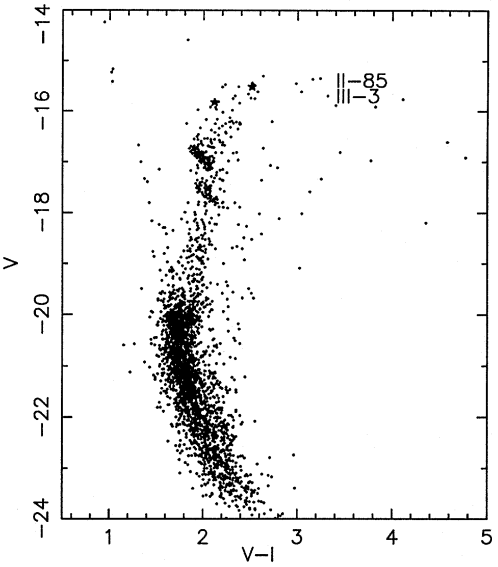

Fig. 2. V vs (V-I) Colour-Magnitude Diagram of NGC 6553 (HST data), where the sample stars are identified.

wavelength region covered is $\lambda\lambda$ 500-750 nm, at a resolution of R $\approx$ 20.000. The reductions were carried out with the routines for échelle spectra contained in the Midas package. This procedure automatically finds the center of the orders, tracks them across the CCD chip and extracts them by summing over a selected input width of pixels. The package allows wavelength calibration by identifying two pairs of lines on the thorium lamp image.

A typical spectrum is shown in Fig. 1 for order 93 of the giant member III-3 and the log of observations is reported in Table 1, where radial velocities derived from several unblended atomic lines in the spectra are indicated. A mean v_r = 6.4 km/s or heliocentric v_r^{hel} = 6.1 km/s is found, compatible with the value of -5 km/s given in Zinn & West (1984) or -12 km/s given in Zinn (1985), and in very good agreement with the value of 8.4 km/s measured by Rutledge et al. (1997a). A S/N $\sim$ 50 was measured at order 88 for both stars.

In Fig. 2 is shown the V vs. (V-I) Colour-Magnitude Diagram of NGC 6553 using our data obtained with the Hubble Space Telescope (Ortolani et al. 1995) where the sample stars are identified. The identification names given in Hartwick (1975) are adopted along the text.

Table 1. Log observations

star	date	UT	exp. (h)	v_r^{obs} km/s	$v_r^{hel.}$ km/s
II-85	24.06.93	5:30	1:15	7.3	7.08
III-3	”	6:50	1:15	5.5	5.11

Table 2. Magnitudes of the program stars

star	V Hart.	B Dan	V Dan	R Dan	I Dan	V HST	I HST	J IRAC	K IRAC
III-3	15.61	17.59	15.42	13.68	13.18	15.83	13.41	11.54	10.33
II-85	15.32	17.38	15.13	13.31	12.73	15.52	13.01	11.04	9.79

3. Stellar parameters

3.1. Temperatures

The crucial issue in the detailed analysis of these cool and metal-rich giants is the determination of their effective temperatures T_{eff}. We obtained very high quality V and I colours using the Hubble Space Telescope (HST) and J and K colours using the detector IRAC2 at the 2.2m telescope of ESO (Ortolani et al. 1995; Guarnieri et al. 1998).

In Table 2 are given the magnitudes: V from Hartwick (1975), BVR from Ortolani et al. (1990), VI from Ortolani et al. (1995) and JK from Guarnieri et al. (1998). It is interesting to note the large offsets in the V magnitudes between Hartwick (1975), Ortolani et al. (1990) and Ortolani et al. (1995) values. This clearly reveals the improvement of the photometry in crowded fields, which occurred along the years from photographic, to ground-based CCD, and HST data. HST calibration of V and I was tied to the Cousins system. The calibration of our old Danish data (Ortolani et al. 1990) showed an offset of about 0.28 mag, very probably due to crowding. A revised calibration of the Ortolani et al. (1990) data done with the more accurate crowding compensation showed excellent agreement with the new HST data.

A further step in the derivation of temperatures, is the reddening value adopted. In Guarnieri et al. (1998) we derived a colour excess of $E(V-I) = 0.95$ for NGC 6553. Assuming a ratio $E(V-I)/E(B-V) = 1.33$ (Dean et al. 1978) the resulting $E(B-V)$ is 0.7. Assuming E(V-K)/E(B-V) = 2.744 and E(J-K)/E(B-V) = 0.527 (Rieke & Lebofsky 1985), the available colours were dereddened. In Table 3 are given the observed and

Table 3. Observed/dereddened colours

star	$(B^D - V^H)$	$(V - I)^H$	$(V^H - K)$	$(J - K)$
III-3	1.76	2.42	5.50	1.21
	1.06	1.47	3.58	0.84
II-85	1.86	2.51	5.73	1.25
	1.16	1.56	3.81	0.88

Table 4. Derived temperatures using relations by McWilliam (1990) and Blackwell & Lynas-Gray (1994), and using Table 5 of Bessell et al. (1998) adopting [Fe/H] = −0.3 and log g = 1.0.

star	T^{Mc}_{B-V}	$T^{Mc}_{(V-I)}$	T^{Mc}_{V-K}	T^{Bl}_{V-K}	T^{Mc}_{J-K}	T^{Bes}_{J-K}	T^{Bes}_{V-K}	T^{Bes}_{V-I}
III-3	4637	4436	3933	4140	4278	4219	3936	3990
II-85	4431	4323	3863	4145	4171	4109	3835	3913

dereddened colours. In order to derive temperatures we used several methods:

(i) Infrared flux method: Based on absolute measurements of stellar monochromatic fluxes in the infrared region for a sample of 80 solar metallicity stars, Blackwell & Lynas-Gray (1994) established the relation T(V-K) = 8862–2583(V-K)–353.1(V-K)^2.

(ii) Relations by McWilliam (1990): Based on a sample of 671 giants of about solar metallicity McWilliam (1990): derived the relations between the (B-V), (V-K), (V-I) and (J-K) colours and effective temperatures. The resulting temperatures obtained with the use of relations (i) and (ii) are given in Table 4; it has to be noted however that in both cases (McWilliam 1990 and Blackwell & Lynas-Gray 1994) the samples on which the relations are based did not contain a significant number of stars with effective temperatures around 4000 K and below, so that such relations should be valid only for Teff $>$ 4000 K, at the edge of validity for our sample stars.

(iii) tables by Bessell et al. (1998): these calibrations based on NMARCS models of Plez (1995, unpublished) were obtained by linear interpolation in their Table 5; these temperatures are also reported in Table 4.

We have adopted Teff = 4000 K for the 2 sample stars, based essentially on the calibrations by Bessell et al. (1998) (Table 4).

3.2. Gravities

The classical relation $\log g_* = 4.44 + 4 \log T_*/T_\odot + 0.4(M_{\rm bol} - 4.74) + \log M_*/M_\odot$ was used (adopting $T_\odot$ = 5770 K, M_* = 0.8 $M_\odot$ and $M_{\rm bol\odot}$ = 4.74 cf. Bessell et al. 1998). For deriving $M_{\rm bol*}$ we adopted M_V(HB) = 1.06 (following Buonanno et al. 1989), V(HB) = 16.92 and E(B-V) = 0.7 (Guarnieri et al. 1998) and bolometric magnitude corrections $BC_V = -0.90$ cf. Bessell et al. (1998); the resulting $M_{\rm bol}$ values are given in Table 6. Due to an overionisation effect, as discussed in Pilachowski et al. (1983), a corrected value for log g, lower by 0.6 dex is adopted (values in parenthesis in Table 6). The ionisation equilibrium with these gravities was checked by verifying if the curves-of-growth of FeI and FeII give the same Fe abundance.

Table 5. Metallicity of NGC 6553 given in the literature. References to Table: 1 Zinn (1980); 2 Bica & Pastoriza (1983); 3 Cohen (1983); 4 Zinn & West (1984); 5 Pilachowski (1984); 6 Webbink (1985); 7 Bica & Alloin (1986); 8 Barbuy et al. (1992); 9 Harris (1996); 10 Origlia et al. (1997); 11 Rutledge et al. (1997b) – the first value corresponds to the Zinn & West (1984) scale and the second one to the Carretta & Gratton (1997) scale; 12 Carretta & Gratton (1997)

[M/H]	reference	method
+0.04	1	integrated Q39 photometry
+0.47	2	integrated DDO photometry
−0.46,−0.33	3	high-res. spectroscopy
−0.29	4	integrated spectroscopy
−0.70	5	high-res. spectroscopy
−0.41	6	compilation
+0.1	7	integrated spectroscopy
−0.20	8	high-res. spectroscopy
−0.25	9	compilation
−0.33	10	CO integrated spectroscopy
−0.18,−0.60	11	mid-res. spectroscopy of giants
−0.60	12	revised met. scale of g.clusters

Table 6. Stellar parameters adopted. The log g values in parenthesis are the corrected values taking into account overionisation effects.

star	$T_{\rm eff}$	$M_{\rm bol}$	log g	[Fe/H]	v_t(km/s)
III-3	4000	−0.935	1.44 (0.8)	−0.6±0.2	1.3
II-85	4000	−1.245	1.26 (0.7)	−0.5±0.2	1.3

3.3. Metallicity

For comparison purposes, in Table 5 are given the metallicity values reported in the literature for NGC 6553, together with indication of the method employed in each case. Notice the spread in the metallicities reported, which we believe can be explained by a combination of overabundances of α-elements, to a moderate metallicity as deduced from Fe lines (Sect. 5).

3.3.1. Model atmospheres

We have adopted the photospheric models for giants of Plez et al. (1992) and their extended grid kindly made available to us by B. Plez (1997, private communication).

3.3.2. Oscillator strengths

We have used two sets of oscillator strengths gfs:

(i) Along the years we have fitted line-by-line the solar spectrum, by comparing synthetic spectra computed with the Holweger & Müller (1974) semi-empirical solar model to the observed solar spectrum at the center of the solar disk Delbouille et al. (1973), in the wavelength range $\lambda\lambda$ 4000–8700 Å (see for example Castro

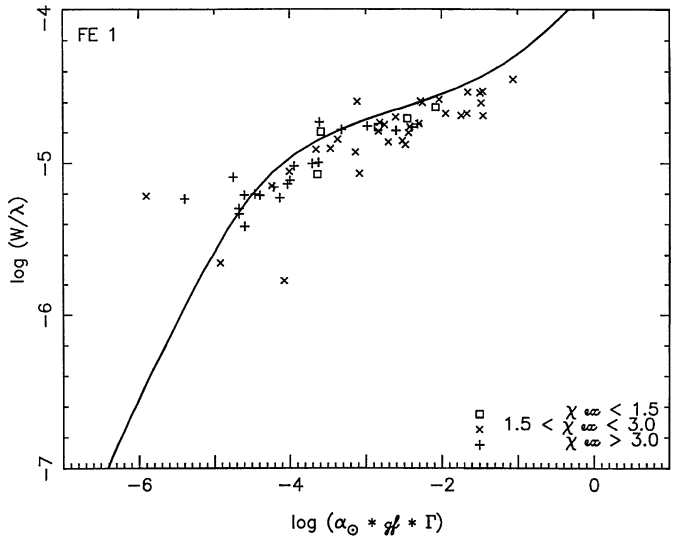

Fig. 3. Curve-of-growth of FeI for the star III-3, using stellar parameters ($T_{\rm eff}$, log g, [Fe/H], v_t) = (4000, 1.0, −0.6, 1.3), and adopting oscillator strengths by Wiese et al.

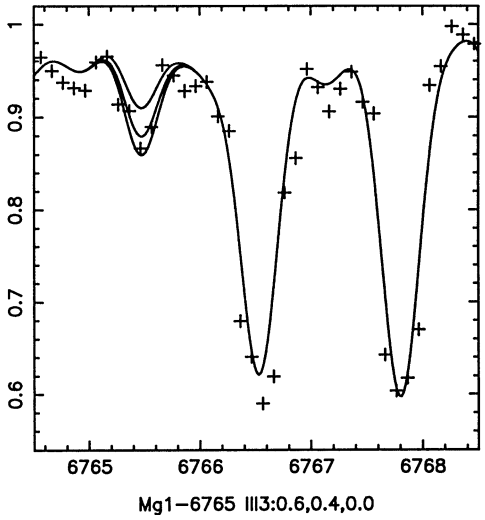

Fig. 4. III-3: MgI λ 6765.450 Å line. Dashed line: observed spectrum; solid lines: synthetic spectra computed with [Mg/Fe] = 0.0, +0.4 and +0.6.

et al. 1995). This work has been carried out with the intent of applying spectrum synthesis to large wavelength regions (e.g. Barbuy 1994), in which case gfs for all lines are needed; we emphasize that there is no complete list of accurate laboratory gf values.

(ii) Laboratory oscillator strengths available in Fuhr et al. (1988), Martin et al. (1988) and Wiese et al. (1969) and compilations of laboratory gf values by MR.

For the curves of growth only the laboratory (ii) gfs were used, since they are more homogeneous, showing less spread. For the spectrum synthesis calculations the laboratory (ii) gfs are used where available, and our fitted gfs (i) are employed for the remaining lines.

3.3.3. Continuum definition

The equivalent widths have been measured using the detectable pseudo-continuum, as illustrated in Fig. 1. This procedure was adopted in order to minimize uncertainties in the equivalent width measurements, from one order to another, due to a non-homogeneous placement of the continuum. On the other hand, when overplotting the theoretical curve-of-growth on the observed points, we considered the upper metallicity envelope, as shown in Fig. 3. The metallicities so derived are reported in Table 6. Such metallicity values were then tested through direct comparison of synthetic to the observed spectra, confirming these values. We note that curves-of-growth computed with $T_{\rm eff}$ = 4250 K give a metallicity of +0.2 dex relative to the values obtained with $T_{\rm eff}$ = 4000 K.

3.3.4. Curves-of-growth

The metallicities were derived by plotting curves of growth of FeI, where the equivalent widths of a selected list of lines were measured using IRAF, and the code RENOIR by M. Spite was employed for plotting the curves of growth. The FeI curve of growth for III-3 is shown in Fig. 3. The final stellar parameters adopted are shown in Table 6. The resulting metallicity for the cluster is [Fe/H] = -0.55 ± 0.2. The difference with respect to Barbuy et al. (1992) where [Fe/H] = -0.2 was derived for the star III-17 can be explained by the main reason that no equivalent widths of FeI had been measured, and only overall fits of synthetic spectra, using the gf's (i) (Sect. 3.3.2) in a region with many blends ($\lambda\lambda$ 5000–6000 Å) were carried out. That procedure was adopted in view of the low S/N of the spectrum, which we had to convolve further reducing the resolution.

3.3.5. Abundance ratios

In Table 7 are reported the lines used, together with oscillator strengths, and the abundance ratios found line-by-line.

The calculations of synthetic spectra were carried out using the code described in Barbuy (1982) where molecular lines of CN $A^2\Pi$-$X^2\Sigma$, C_2 $A^3\Pi$-$X^3\Pi$ and TiO $A^3\Phi$-$X^3\Delta$ γ system are taken into account.

Abundance ratios were derived by computing synthetic spectra line-by-line. For this we have adopted laboratory gf-values (Sect. 3.3.2) for the lines studied. By the use of an homogeneous set of oscillator strengths, the abundance ratios present very low uncertainties.

In Figs. 4 to 10 are shown fits of synthetic to observed spectra for some of the lines indicated in Table 7.

In Table 8 are given the final mean values of the abundance ratios.

4. Discussion

The main results for the two stars (III-3 and II-85) that we have analysed can be summarized as follows:

Table 7. Line by line abundance ratios. Oscillator strengths values refer to 'fit' = our fitting to the solar spectrum (Sect. 3.3.2); 'MR' – McWilliam & Rich 1994; 'W' = Wiese et al. 1969, Fuhr et al. 1988 and Martin et al. 1988

species	λ (A)	$\chi_{\rm ex}$	loggf$^{\rm fit}$	loggf$^{\rm MR}$	loggf$^{\rm W}$	[X/Fe] III − 3	[X/Fe] II − 85
[Fe/H]						−0.6	−0.5
NaI	6154.230	2.10	−1.550	−1.570	−1.560	+0.6	+0.6
NaI	6160.753	2.10	−1.250	−1.270	−1.261	+0.8	+0.6
MgI	6319.242	5.11	−2.200	−2.215	–	+0.4	+0.2
MgI	6765.450	5.75	−1.950	−1.940	–	+0.5	–
MgI	7387.700	5.75	−1.146	−0.870	–	+0.5	+0.2
AlI	6696.032	3.14	−1.610	−1.481	−1.343	+0.6	+0.4
AlI	6698.669	3.14	−1.900	−1.782	−1.650	+0.6	+0.4
SiI	6237.328	5.61	−2.160	−1.010	–	+0.4	+0.3
SiI	6721.844	5.86	−1.230	−1.169	−0.940	+0.4	+0.4
SiI	7405.790	5.61	−0.630	−0.660	–	+0.4	+0.2
CaI	6156.030	2.52	−2.690	–	−2.200	+0.5	+0.4
CaI	6166.440	2.52	−0.980	−1.142	−0.900	+0.4	0.0
CaI	6169.044	2.52	−0.500	−0.797	−0.550	+0.4	+0.1
CaI	6169.564	2.52	−0.180	−0.478	−0.270	+0.4	+0.2
CaI	6455.605	2.52	−1.280	−1.290	−1.350	+0.4	–
CaI	6508.846	2.52	−2.570	−2.500	−2.110	+0.4	0.0
CaI	6717.687	2.71	−0.250	–	−0.610	+0.6	+0.4
TiI	6303.767	1.44	−1.700	−1.566	−1.566	+0.6	+0.6
TiI	6336.113	1.44	−1.840	−1.743	−1.743	+0.6	+0.4
TiI	6508.154	1.43	−3.000	−2.050	–	–	+0.4
TiI	6554.238	1.44	−1.360	−1.218	−1.218	+0.6	+0.4
TiI	6556.077	1.46	−1.200	−1.074	−1.074	+0.6	+0.4
TiI	6743.127	0.90	−1.700	−1.630	−1.630	+0.6	+0.2
TiI	6861.500	2.27	−0.740	−0.740	−0.740	–	+0.2
TiI	7209.468	1.46	−0.330	−0.500	−0.500	$>$ +0.6	+0.6
TiI	7216.190	1.44	−1.160	−1.150	−1.150	$>$ +0.6	+0.6
TiII	6559.576	2.05	−3.360	−2.480	–	+0.6	+0.1
TiII	7214.741	2.59	−1.900	−1.740	−1.740	+0.2	+0.1
YI	6435.049	0.070	−0.760	−0.820	–	+0.4	0.0
YII	6795.410	1.73	−1.250	−1.250	–	+0.3	0.0
YII	7450.320	1.75	−1.530	−0.780	–	0.0	0.0
ZrI	6762.398	0.00	−1.300	−1.180	–	−0.4	−0.4
BaII	6141.727	0.70	−0.077	−0.077	–	0.0	−0.4
BaII	6496.908	0.60	−0.377	−0.377	–	+0.4	−0.4
LaII	6390.480	0.32	−1.520	−1.520	–	+0.4	0.0
LaII	6774.260	0.13	−1.810	−1.810	–	0.0	+0.1
EuII	6645.127	1.38	−0.097	+0.204	–	0.0	0.0

1. Iron is a factor ~ 3.5 subsolar.
2. The α-elements Mg, Si, Ca, Ti are enhanced relative to iron by ~ 0.35 dex.
3. The odd-Z elements Na and Al that are built during carbon burning are enhanced.
4. The s-process elements Y, Zr, Ba, La do not show a systematic trend, some appear to be enhanced, some depleted compared to iron.
5. The r-process element Eu is solar compared to iron.

This general pattern is consistent with the one exhibited by inner halo globular clusters of comparable metallicity, see e.g. Table 1 in Wheeler, Sneden, Truran (1989) for [Fe/H]$\simeq -0.8$ clusters. An overabundance of α-elements relative to iron is now generally interpreted as evidence of **fast** chemical enrichment. Under such circumstances stars form out of an ISM that was enriched predominantly by short lived massive stars exploding as SNs of Type II, before the explosion of most SNs of Type Ia belonging to the same generation(s). This interpretation applies to the well known α-element overabundance in the galactic Halo, as well as to a possible overabundance in elliptical galaxies (e.g. Davies et al. 1993).

Models of bulge formation in which much of the stellar build up is completed in a time shorter than the assumed time for the bulk of SNIa products to be released naturally produce an α-element enhancement (e.g. Matteucci & Brocato 1990). Besides depending on the theoretical SN yields, the detailed abundance pattern predicted by these models is mainly controlled by the

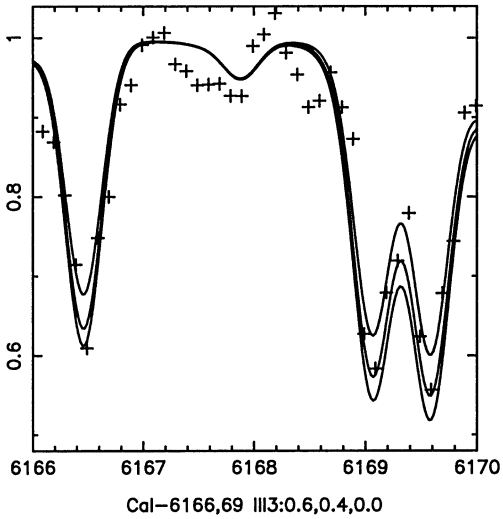

Fig. 5. III-3: CaI λ 6166.440, 6169.044, 6169.564 Å lines. Dashed line: observed spectrum; solid lines: synthetic spectra computed with [Ca/Fe] = 0.0, +0.4 and +0.6.

Table 8. Final mean abundance ratios

	III − 3	III − 3	II − 85	II − 85	
species	no. lines	[X/Fe]	no. lines	[X/Fe]	Mean
NaI	2	+0.7	2	+0.6	+0.65
MgI	3	+0.45	2	+0.2	+0.33
AlI	2	+0.6	2	+0.4	+0.50
SiI	3	+0.4	3	+0.3	+0.35
CaI	7	+0.44	6	+0.2	+0.32
TiI	7	+0.6	9	+0.42	+0.50
TiII	2	+0.4	2	+0.1	+0.25
YI	1	+0.4	1	0.0	+0.20
YII	2	+0.15	2	0.0	+0.07
ZrI	1	−0.4	1	−0.4	−0.40
BaII	2	+0.2	2	−0.4	−0.10
LaII	2	+0.2	2	+0.05	+0.13
EuII	1	0.0	1	0.0	0.0

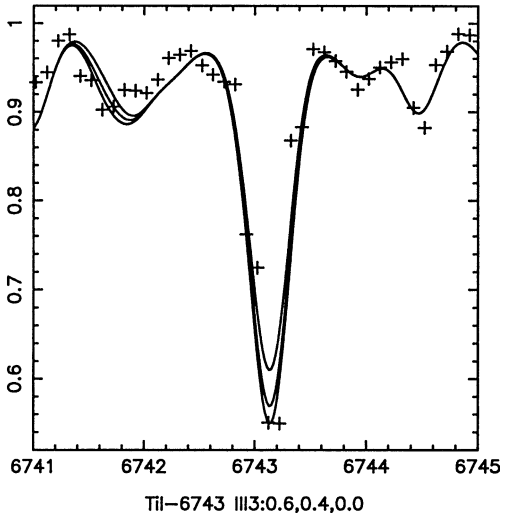

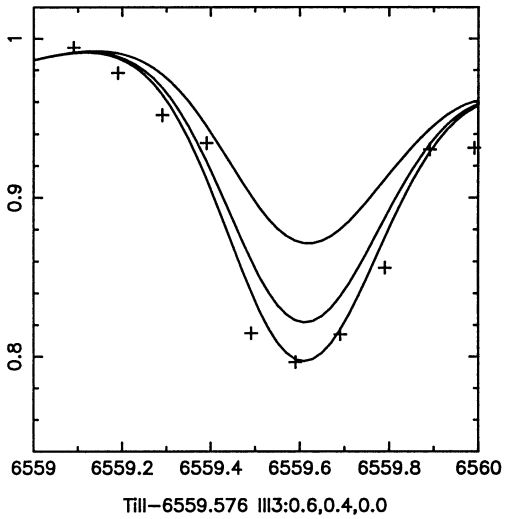

Fig. 6a and b. III-3: **a** TiI λ 6743.127 Å line. Dashed line: observed spectrum; solid lines: synthetic spectra computed with [Ti/Fe] = 0.0, +0.4 and +0.6. **b** TiII λ 6559.576 Å line. Same as in **a**.

ratio of the two relevant timescales: the star formation timescale and the timescale for the bulk (e.g. 50%) of the SNIa products to be released. Fitting to an observed set of elemental abundances allows to recover this ratio, i.e. the star formation timescale is derived modulo the SNIa timescale. While this latter timescale is generally considered to be of the order of 1 Gyr, it is worth recalling that no firm theoretical or observational limit exists on this quantity (e.g. Greggio 1996).

The situation is more confused as far as the s-process elements are concerned. First of all, none of the elements for which we have obtained the abundance is a pure s-process element, but some r-process contribution is also present. Second, some s-processing takes place in massive stars (Raiteri et al. 1993), as well as in relatively short lived and long lived intermediate mass stars (Gallino et al. 1998). In any event, when referring to α-elements the s-process elements are underabundant with respect to the sun, i.e. [s/α] < 0, which also argues for the bulge material out of which NGC 6553 formed having failed to experience enrichment by long lived stars.

All in all, we can notice that the elemental abundances in the two program stars favor a scenario in which the galactic bulge underwent a rapid chemical enrichment, as indeed indicated also by the old age of NGC 6553, and by the small age dispersion of bulge stars as inferred from their luminosity function (Ortolani et al. 1995).

5. Conclusions

We have determined a metallicity of [Fe/H] = -0.55 ± 0.2 for NGC 6553, together with an overabundance of α-elements, as well as of Na and Al, in the range +0.3 $<$ [X/Fe] $<$ +0.6 (Table 8). Using the overabundances given in Table 8, and assuming [O/Fe] = [S/Fe] = [Ne/Fe] = +0.4 (as we would expect from the overabundances obtained for the other α-elements), we obtain an overall content in heavy elements of Z = 0.014, or

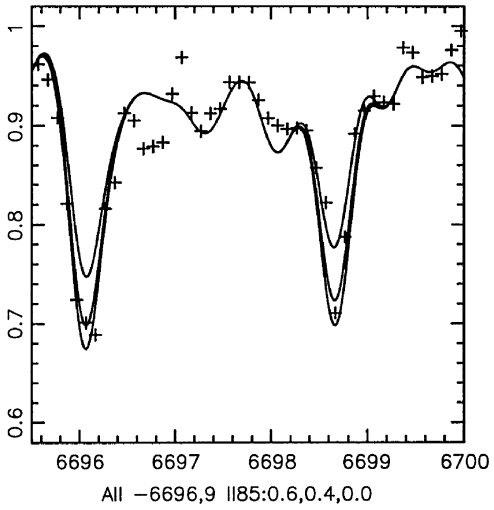

Fig. 7. II-85: AlI λ 6696.032, 6698.669 Å lines. Dashed line: observed spectrum; solid lines: synthetic spectra computed with [Al/Fe] = 0.0, +0.4 and +0.6.

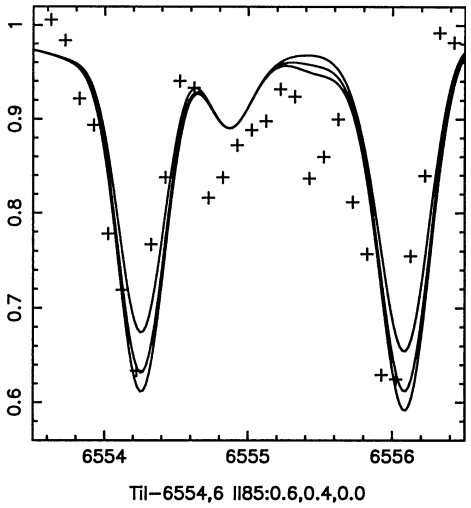

Fig. 8. II-85: TiI λ 6554.238, 6556.077 Å lines. Dashed line: observed spectrum; solid lines: synthetic spectra computed with [Ti/Fe] = 0.0, +0.4 and +0.6.

[Z/Z$_\odot$] = −0.08, which is almost solar. This is likely to explain why integrated observations tend to give a higher metallicity to NGC 6553, relative to high-resolution observations of FeI lines. As a reference for the metallicity scale of globular clusters, let us point out that [Z/Z$_\odot$] = −0.32 for 47 Tuc (Brown et al. 1990; Brown & Wallerstein 1992). The formal difference is only ~ 0.24 dex, and yet the red giant branch of NGC 6553 climbs only ~ 1 magnitude in V above the horizontal branch, while in 47 Tuc it climbs more than two magnitudes above the horizontal branch (Ortolani et al. 1995). This indicates that the TiO blanketing in the V band is much stronger in NGC 6553 red giants compared to 47 Tuc. At least in part, such a very high sensitivity is likely to be due to both Ti and O being enhanced in NGC 6553, with the abundance of the TiO molecule being proportional to the product of the two abundances.

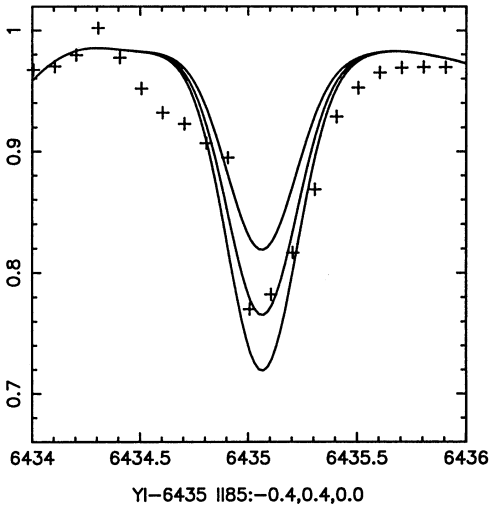

Fig. 9. II-85: YI λ 6435.049 Å line. Dashed line: observed spectrum; solid lines: synthetic spectra computed with [Y/Fe] = −0.4, 0.0 and +0.4.

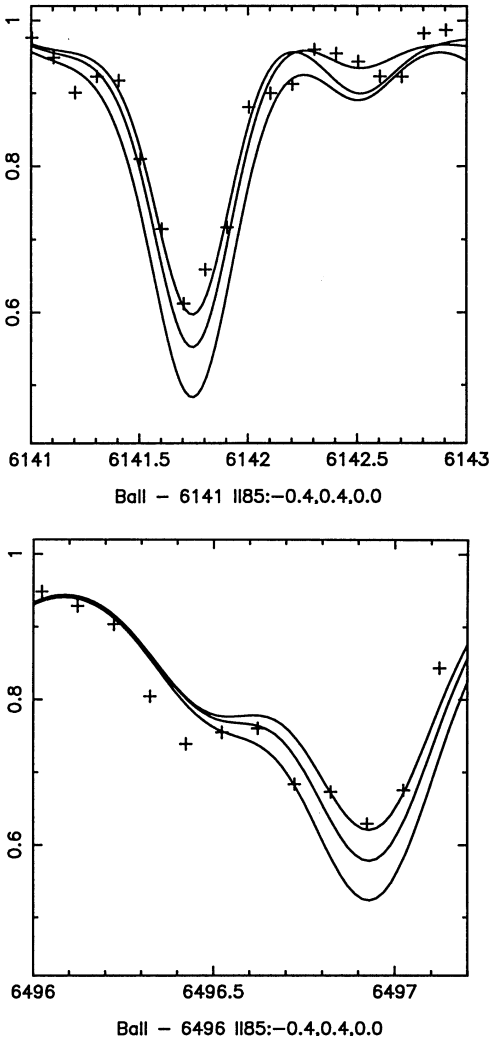

Fig. 10a and b II-85: **a** BaII λ 6141.727 Å line. Dashed line: observed spectrum; solid lines: synthetic spectra computed with [Ba/Fe] = −0.4, 0.0 and +0.4. **b** BaII λ 6496.910 Å line. Same as in **a**.

The abundance ratios in the program stars indicate that the chemical enrichment of the gas from which the bulge cluster NGC 6553 formed was dominated by Type II SNs, with little contamination from long lived stars such as the precursors of Type Ia SNs. Therefore, these findings favour a scenario in which the bulge underwent rapid star formation and chemical enrichment, as also indicated by the colour magnitude diagrams and luminosity functions of bulge globulars and bulge field populations (Ortolani et al. 1995).

Together with the evidence for old stellar populations being dominant in galactic spheroids (ellipticals and bulges), the evidence presented in this paper lends further support to the notion of a much higher star formation rate in the early universe ($z > 3$) compared to the present-day universe (Renzini 1998).

Acknowledgements. We acknowledge partial financial support from CNPq and Fapesp (Brazil).

References

Barbuy B., 1982, PhD thesis, Université de Paris VII
Barbuy B., 1994, ApJ 430, 218
Barbuy B., Bica E., Ortolani S., 1998, A&A 333, 117
Barbuy B., Castro S., Ortolani S., Bica E., 1992, A&A 259, 607
Bessell M.S., Castelli F., Plez B., 1998, A&A 333, 231
Bica E., Alloin D., 1986, A&A 162, 21
Bica E., Pastoriza M., 1983, ASSci 91, 99
Bica E., Barbuy B., Ortolani S., 1991, ApJ 382, L15
Blackwell D.E., Lynas-Gray A.E., 1994, A&A 282, 899
Brown J.A., Wallerstein G., Oke J.B., 1990, AJ, 100, 1561
Brown J.A., Wallerstein G., 1992, AJ 104, 1818
Buonanno R., Corsi C.E., Fusi-Pecci F., 1989, A&A 216, 80
Carretta E., Gratton R.G., 1997, A&AS 121, 95
Castro S., Barbuy B., Bica E., Ortolani S., Renzini A., 1995, A&AS 111, 17
Cohen J.G., 1983, ApJ 270, 654
Davies R.L., Sadler E.M., Peletier R.F., 1993, MNRAS 262, 650
Dean J.F., Warpen P.R., Cousins A.J., 1978, MNRAS 183, 569
Delbouille L., Roland G., Neven L., 1973, Photometric Atlas of the Solar Spectrum from 3000 to 10000 Å, Liège
Guarnieri M.D., Ortolani S., Montegriffo P., et al.,A&A 331, 70
Fuhr J.R., Martin G.A., Wiese W.L., 1988, Atomic Transition Probabilities: Iron through Nickel, Journal of Physical and Chemical Reference Data vol. 17, suppl. no. 4
Gallino R., et al., 1998, ApJ 497, 388
Greggio L., 1996, In: Kunth D., et al. (eds.) Interplay Between Massive Star Formation, the ISM and Galaxy Evolution, Edition frontieres, Gyf sur Yvette, p. 89
Harris W.E., 1996, AJ 112 1487
Hartwick F.D.A., 1975, PASP 87, 77
Holweger H., Müller E., 1974, Solar Phys. 39, 19
Idiart T., Freitas Pacheco J.A., Costa R.D.D., 1996, AJ 111, 1169
Martin G.A., Fuhr J.R., Wiese W.L., 1988, Atomic Transition Probabilities: Scandium through Manganese, Journal of Physical and Chemical Reference Data vol. 17, suppl. no. 3
Matteucci F., Brocato E., 1990, ApJ 365, 539
McWilliam A., 1990, ApJS 74, 1075
McWilliam A., Rich R.M., 1994, ApJS 91, 749 (MR)
Origlia L., Ferraro F.R., Fusi Pecci F., Oliva E., 1997, A&A 321, 859
Ortolani S., Barbuy B., Bica E., 1990, A&A 236, 362
Ortolani S., Renzini A., Gilmozzi R., et al., 1995, Nature 377, 701
Plez B., Brett J.M., Nordlund, 1992, A&A 256, 551
Pilachowski C.A., Sneden C., Wallerstein G. 1983, ApJS 273, 187
Pilachowski C.A., 1984, ApJ 281, 614
Raiteri C.M., Gallino R., Busso M., Neuberger D., Käppeler F., 1993, ApJ 419, 207
Renzini A., 1998, astro-ph/9801209, In: D'Odorico S., Fontana A., Giallongo E. (eds.) The Young Universe, ASP Conf. Ser. 146, 298
Rieke G.H., Lebofsky M.J., 1985, ApJ 288, 618
Rutledge G.A., Hesser J.E., Stetson P.B., et al., 1997a, PASP 109, 883
Rutledge G.A., Hesser J.E., Stetson P.B., 1997b, PASP 109, 907
Sadler E.M., Terndrup D.M., Rich R.M., 1996, AJ 112, 117
Webbink R.F., 1985, In: Goodman J., Hut P. (eds.) Dynamics of Star Clusters, IAU Symp. 113 (Dordrecht: Reidel), p. 541
Wheeler J.C., Sneden C., Truran J.W., 1989, ARA&A 27, 279
Wiese W.L., Martin G.A., Fuhr J.R., 1969, Atomic Transition Probabilities: Sodium through Calcium, NSRDS-NBS 22
Zinn R., 1980, ApJS 42, 19
Zinn R., 1985, ApJ 293, 424
Zinn R., West M.J., 1984, ApJS 55, 45